

# Persistent currents in carbon nanotubes based rings

Sylvain Latil

G D P C , Université Montpellier II, France

Stephan Roche

Commissariat à l'Energie Atomique,  
D S M /D R F M C /S P S M S , Grenoble, France

Angel Rubio

Departamento de Física de Materiales,  
Facultad de Ciencias Químicas, UPV/EHU,  
and Donostia International Physics Center (DIPC),  
San Sebastian/Donostia, Spain

January 11, 2022

## Abstract

Persistent currents in rings constructed from carbon nanotubes are investigated theoretically. After studying the contribution of finite temperature or quenched disorder on covalent rings, the complexity due to the bundle packing is addressed. The case of interacting nanotori and self-interacting coiled nanotubes are analyzed in details in relation with experiments.

## I Introduction and background

Carbon nanotubes are micrometer-long hollow cylinders with nanometer scale radius, and electronic properties strongly depending on their geometrical helicity [1]. As promising tools for building up nanoscale electronic devices [2, 3], nanotubes also allow to challenge the well established common theories of mesoscopic physics. Recently, many works of quantum transport in these systems have revealed puzzling properties resulting from the mixing between their nanometer and micrometer combined length scales [4, 5, 6, 7, 8].

Nanotubes are very particular in the sense that they lie in between small molecular systems such as benzene-type ring molecules, and mesoscopic systems

---

Present address: Unite PCPM, Université Catholique de Louvain, Louvain-la-Neuve, Belgium

such as metallic or semiconducting wires. In the former entities, basic electronic conduction properties are entirely monitored by HOMO-LUMO gap and discrete features of the spectrum, whereas quantum wires may manifest, apart from ballistic transport, band conduction allowing quantum interference phenomena whenever full coherence of the wave function is maintained over a reasonable scale.

In metallic single wall nanotubes, at the charge neutrality point there exists some evidence of a Luttinger liquid behavior, namely that electron-electron interactions are strong enough to deviate the electronic status from Fermi liquid [9]. Besides, a recent work shows that the tube-tube interaction between different nanotube layers is able to induce a transition from the Luttinger liquid to a strongly correlated Fermi system or a Fermi liquid [10]. However, other results on scanning tunneling spectroscopy [11] are fully interpreted in terms of the independent electrons model indicating the importance of screening effects.

Rings of single-walled carbon nanotubes have been synthesized experimentally [12, 13]. Depending on the circumference length of the ring, a transition from n-type semiconducting to metallic behavior was observed experimentally (from 60 nm to 1 μm) [14] and further discussed theoretically [15]. Magnetotransport experiments on rings have also been performed [16], manifesting negative magnetoresistance and weak electron-electron interactions in the low temperature regime. However, no clear Aharonov-Bohm effect was found, in opposition with the properties of multiwalled nanotubes (MWNTs) case [17, 18].

An applied magnetic flux is known to induce ring currents in molecules [19], and persistent currents (PC) in mesoscopic rings [20]. In fact, every thermodynamic functions of the system are  $\Phi_0$ -periodic functions of the flux, where  $\Phi_0 = h/e$  is the flux quantum. Investigation of PC then yields valuable information to understand both quantum coherence and dephasing rates [21, 22]. These non dissipative currents are intimately related with the nature of eigenfunctions of isolated rings and their flux sensitivity [20]. The manifestation of  $\Phi_0$  periodic oscillations of magnetoresistance or persistent currents is a generic feature that depends on the degree of disorder and employed averaging procedure [20, 21]. Let us introduce a dimensionless flux  $\varphi = \Phi/\Phi_0$ . For non-interacting electrons, the total current at zero temperature is calculated by the following expression :

$$I_{pc} = \sum_n \frac{\partial \epsilon_n}{\partial \varphi} = \frac{1}{\Phi_0} \sum_n \frac{\partial \epsilon_n}{\partial \varphi} \quad (1)$$

with the summation running up to the last occupied energy levels. At finite temperature  $T$ , all the states participate formally to the total free energy, and

$$I_{pc}(T) = \frac{1}{\Phi_0} \sum_n \frac{\partial f_n}{\partial \varphi} \quad (2)$$

with

$$f_n = \frac{1}{1 + \exp \left( \frac{\epsilon_n - \mu}{k_B T} \right)} \quad (3)$$

where  $\epsilon_F$  is the Fermi level, and  $k_B$  the Boltzmann constant. In ballistic mesoscopic rings, perfect agreement between theory and experiments has been reported [23], differently to disusive systems (i.e. the mean free path  $l_e$  becomes smaller than the ring circumference  $L_{\text{ring}}$ ), for which the discrepancy between the theoretical and the experimental values of PC ( $I_{\text{pc}}^{\text{theor}} \sim 10^{-2} I_{\text{pc}}^{\text{exp}}$ ) remains an open controversy, with electron-electron interactions [24, 25], confinement effects [26] or non-equilibrium phenomenon [22] as possible explanations. Persistent currents in a Luttinger liquid has been analyzed in [27].

The goal of the present work is to establish to which extent the intrinsic features of carbon nanotubes based ring geometries (helicities of individual tubes, tube-tube interaction, ...) are reflected on the persistent current patterns in the coherent regime, neglecting electron-electron interactions.

## II Persistent currents in a simple carbon torus

Different works have been published recently on the magnetic properties of simple carbon tori [28, 29], both are formally based on a tight-binding (TB) approach. In this paper, the same model is used. It consists in a finite length  $(n; m)$  nanotube (containing  $N$  primitive cells) curled up onto a torus. Such torus will be named like  $(n; m) \times N$ . If the circumference  $L_{\text{ring}}$  of the torus is long enough, the effect of the curvature on the electronic properties is weak and the topologically equivalent system of a straight nanotube with periodic boundary conditions keeps the essential physics. The band structure of this straight tube is calculated with the zone folding technique [1], keeping only one electron per site and assuming a constant hopping  $t_0$  between the first neighboring sites. The resulting flux dependent hamiltonian is

$$H = \sum_{i,j \in (i)} \sum_{\alpha} \psi_{i\alpha}^\dagger \psi_{j\alpha} \exp(i\phi'_{ij}) \quad (4)$$

$$\phi'_{ij} = 2\pi \left( \frac{z_j - z_i}{L_{\text{ring}}} \right) \quad (5)$$

where  $\psi_{i\alpha}$  and  $\psi_{j\alpha}$  are the  $\alpha$ -orbitals located on site, whose positions along tube axis are called  $z_i$  and  $z_j$ , and  $\phi = \phi_0$  is the dimensionless magnetic flux. Since the ring contains  $N$  primitive cells, the first Brillouin zone is sampled for a number  $N$  of  $k$ -points, equally separated by  $k = 2\pi/L_{\text{ring}}$ , and the linearization of the band structure near the Fermi points implies that the energy level spacing is  $\epsilon_F = \hbar v_F = L_{\text{ring}}$ . In this case, the magnetic flux through the ring acts just as a dephasing rate on the electronic levels, i.e. the sampling of  $k$  points in the first Brillouin zone is shifted about  $k = k_0 + \phi/\phi_0$ .

As reported by Lin and Chuu [28], there are two kinds of metallic carbon tori. If the Fermi momentum is zero, or if the number  $N$  of cells is a multiple of 3, then the torus possesses a vanishing HOMO-LUMO gap at zero field (type I). If the Fermi momentum is non zero, and the number of cells is not a multiple of 3, then the torus is sorted onto type II, with a non vanishing gap at zero

eld. On the other hand, a semiconducting carbon torus do not exhibit any flux dependent effect [30].

The physical origin of the persistent currents is the cyclic boundary condition of the electronic system, leading to a sampling of  $k$ -points in the Brillouin zone. FIG .1 (left) shows this sampling in the vicinity of the Fermi energy, and the resulting discrete spectrum of electronic levels. The application of a magnetic flux dephases the sampling and moves linearly these levels (Zeeman effect) because each  $k$ -point is related to a magnetic momentum. The linear  $\phi$ -dependence of the individual levels is shown in FIG .1 (right). The resulting persistent current  $I_{pc}(\phi)$ , obtain by summing the contribution of each occupied level, is a set of a ne functions of the magnetic flux, as shown on FIG 2. For the type I with  $T = 0$ , it is:

$$I_{pc}(\phi) = I_0 \left( \frac{\phi}{\phi_0} - 2 \right); \quad \frac{\phi}{\phi_0} \in [1; 2] \quad (6)$$

$$I_{pc}(\phi) = I_0 \left( 1 - \frac{\phi}{\phi_0} \right); \quad \frac{\phi}{\phi_0} \in [0; 1] \quad (7)$$

and for the type II:

$$I_{pc}(\phi) = I_0 \left( \frac{\phi}{\phi_0} - 2 \right); \quad \frac{\phi}{\phi_0} \in [1; 3] \quad (8)$$

$$I_{pc}(\phi) = -2I_0; \quad \frac{\phi}{\phi_0} \in [3; 4] \quad (9)$$

$$I_{pc}(\phi) = I_0 \left( 1 - \frac{\phi}{\phi_0} \right); \quad \frac{\phi}{\phi_0} \in [3; 4] \quad (10)$$

with the value  $I_0$  given by

$$I_0 = 2N_c e v_F / L_{ring} \quad (11)$$

with  $N_c$  the number of available channels at Fermi level;  $N_c = 2$  for metallic nanotubes. Hence, the slope of the function  $I_{pc}$  for metallic carbon nanotube is determined by its length only. The reason why the function  $I_{pc}$  is not analytical at the points  $\phi = 0$  and  $\phi = 1\phi_0$  is a crossing of eigenenergies at Fermi level (on FIG .1 right), which provokes a sharp diamagnetic-paramagnetic transition. This work is mainly devoted to the first category of carbon nanotube.

Since  $I_{pc}(\phi)$  is a periodic and odd function, it can be written down as a Fourier series like :

$$I_{pc}(\phi) = \sum_{n=0}^{\infty} b_n \sin(2\pi n \frac{\phi}{\phi_0}) \quad (12)$$

with  $b_n$  the  $n^{th}$  harmonic

$$b_n = 2 \int_0^{\phi_0} I_{pc}(\phi) \sin(2\pi n \frac{\phi}{\phi_0}) d\phi \quad (13)$$

### III Effect of Temperature and disorder

In order to investigate the evolution of  $I_{pc}$ , with different physical parameters, such as static disorder or electronic temperature, the behavior of two typical

currents is analyzed hereafter. The first one is the quadratic flux-averaged current

$$J_{\text{quad}} = \frac{S}{Z_{+1=2}} \int_{1=2} I_{\text{pc}}^2(\phi) d\phi \quad (14)$$

and the second is the absolute value of  $I_{\text{pc}}$  for the quarter of the quantum flux, which is related to the intensity of the first harmonic

$$J_{1=4} = I_{\text{pc}} \frac{1}{4} \quad (15)$$

We first analyze the effect of temperature on the intensity of PCs. Here, we still assume that the phase coherence length  $L_\phi$  is much larger than  $L_{\text{ring}}$ , so that the system remains fully described by the eigenfunctions of its hamiltonian. The electrons are independent and the effect of temperature is to induce a distribution of the occupancy around  $\epsilon_F$ , within  $k_B T$ .  $I_{\text{pc}}(\phi)$  is given by (2). As shown in the left part of FIG 3, the effect of  $T$  is a smoothing of the sawtooth shape of the PCs, which became fully analytical functions. This means that the harmonics of higher order are the first to be affected by temperature. On the right side of FIG 3 is plotted the evolution of the typical currents versus the temperature. The behavior is simple : below a critical temperature  $T_c$  the function  $J_{\text{quad}}$  decreases slightly and  $J_{1=4}$  is a constant. Above the transition, both are exponentially damped. The effect of  $T$  on the PC of linear chains or 1D free electrons systems has been investigated by Cheung et al.[31], who demonstrated that for every shape of band structure, a temperature transition can be defined as:

$$T_c = \frac{E_F}{2} \quad (16)$$

where  $E_F = \hbar v_F / L_{\text{ring}}$  is the level spacing at Fermi energy. When  $T > T_c$  the function  $I_{\text{pc}}(\phi)$  is fairly approximated by its first harmonic, and since this harmonic is the last to be affected, the typical currents decrease drastically after the transition.

It is worth to note that the behavior of such tubular system is exactly the same that a linear chain or 1D free electrons systems. This effect is due to the small number of channels available in a carbon nanotube ( $N_c = 2$ ). In fact, none effect of the radius of the nanotube happens. In that sense, defect free metallic nanotubes behave like real one dimensional systems.

We turn now to the analysis of the effect of a quenched disorder on the persistent current, with a particular focus on the typical value of the averaged current, in order to compare the results with established theories. To discuss the effect of conduction mechanism on persistent currents, static disorder is simulated by a random modulation of the on-site energies [32]. Particular attention is paid to the behavior of PC close to the transition between ballistic and more localized conduction regimes. Since the application of this static disorder breaks the translational symmetry, the whole structure (and no longer one unit cell only) is conserved to solve the eigenproblem. As a generic case of metallic tubes the (6;6) arm chair nanotube (radius  $R = 2.58 \text{ nm}$ ) is considered. The length of the

tube is 75 unit cells, implying a perimeter of about  $L_{\text{ring}} \approx 18.4 \text{ nm}$ , and a single particle level spacing at Fermi energy  $\epsilon_F \approx 0.205 \text{ eV}$ . Randomly fluctuating on-site energies are added to the former  $\delta$ -dependent TB Hamiltonian (4) like

$$H = \sum_i \epsilon(i) \tilde{c}_i^\dagger \tilde{c}_i + \sum_{i,j(i)} t_{ij} \tilde{c}_i^\dagger \tilde{c}_j \exp(i\phi_{ij}) \quad (17)$$

where  $\phi_{ij}$  is given by (5), and  $\epsilon(i)$  is the randomly modulated on-site energy of the  $i^{\text{th}}$  atom. The range of the on-site energies fluctuation is  $[-W, W]$ , where  $W$  is the disorder strength. This modulation enables to tune an important physical transport length scale in nanotubes, namely the electronic mean free path which given by (for the arm chair  $(n, n)$  nanotubes [4, 5])

$$l_e \approx \frac{v_F}{6} \frac{1}{3na_{\text{cc}}} \frac{1}{W} \quad (18)$$

where  $a_{\text{cc}} = 1.42 \text{ \AA}$  is the distance between two carbon atoms of the honeycomb lattice. Since this formula derives from the Fermi golden rule, it should be valid in the limit of weak scattering and for Fermi energies close to the charge neutrality point. An important feature, which is not common in mesoscopic wires, is that, in first approximation, the mean free path scales with the diameter.

In mesoscopic systems, the quantity  $l_e$  discriminates between three different physical conduction regimes: the ballistic motion for  $l_e > L_{\text{ring}}$ , the diffusive regime  $l_e < L_{\text{ring}}$  and the localized regime whenever  $\epsilon_F N_c l_e < L_{\text{ring}}$  [33]. A single level of energy  $\epsilon_n$  carry a current  $I_n^2(\epsilon)$ . In the diffusive regimes of mesoscopic systems, the typical current carried by this single level  $J_{\text{typ}}^{(n)}$  reads [31, 34, 35]

$$J_{\text{typ}}^{(n)} = \frac{q}{h} \frac{I_n^2(\epsilon)}{I_n^2(\epsilon)} \frac{1}{L_{\text{ring}}} \frac{E_c}{0} \quad (19)$$

where  $\overline{I_n^2(\epsilon)}$  denotes the average value over disorder strength and system length, and  $I_n^2(\epsilon)$  is the flux-average current. The typical total current has been found to be in order of

$$J_{\text{typ}} = \sum_n J_{\text{typ}}^{(n)} \frac{E_c}{0} = \frac{ev_F l_e}{L_{\text{ring}}^2} \quad (20)$$

where  $E_c = \hbar D = L_{\text{ring}}^2 = \hbar v_F l_e = L_{\text{ring}}^2$  is the Thouless energy (diffusivity constant is  $D$ ). Differently, the effect of disorder on persistent current remains a complex non-elucidated problem in the ballistic limit [36].

To extract the effect of disorder on persistent currents, we thus follow their  $W$ -dependence. A first observation is that both behaviors of  $J_{\text{quad}}$  and  $J_{1=4}$  are reminiscent to the temperature dependent patterns. We plot the  $W$ -dependence of the two typical currents on FIG. 4a), for a number of random disorder configurations, and the resulting average. The behavior of  $J_{1=4}$  is particularly illustrative since its  $W$  dependence is mainly dominated by the first harmonic. We also plot on FIG. 4b) the dependence of  $J_{\text{quad}}$  and  $J_{1=4}$  upon the equivalent mean free path  $l_e(W)$ , that is given by equation (18). Both are exponentially damped as soon as  $2l_e < L_{\text{ring}}$  which corresponds to  $W \approx 1.83 \times 10^{-4}$ .

For smaller disorder, behaviors become more difficult to interpret within the framework of conventional theory. For a disusive regime, one would expect an averaged persistent current following  $\langle J \rangle = J_0 \frac{L_e}{L_{\text{ring}}}$  so reduced by a factor of  $L_e/L_{\text{ring}}$  with respect to the ballistic case. This would yield a  $(\phi_0/W)^2$  dependence of the amplitude with disorder strength. However, from our results, the damping of  $J_{1=4}$  and  $J_{\text{quad}}$  are much smaller especially for  $L_e < L_{\text{ring}}$ . It is indeed rather difficult to extract the  $W$ -dependence in the ballistic regime, since all harmonics respond differently to a given disorder strength. Actually, as long as  $nL_{\text{ring}} < L_e$ , the harmonic of rank  $n$  remains nearly unaffected by disorder, whereas harmonics with  $nL_{\text{ring}} > 2L_e$  are exponentially damped.

In conclusion except from strong disorder cases, persistent currents in covalent rings of carbon nanotubes are weakly sensitive to disorder and their amplitude remain close to that of the clean ballistic case.

## IV From a simple torus to a bundle

The systems studied in the preceding sections are useful to understand the physical phenomena in carbon nanotubes, but seem far to be a reliable representation for describing the full complexity of nanotube based rings. The bonding nature of the closing of the ring of SWNTs has been suggested either to be covalent [12] or of Van der Waals type [13]. In any case, the synthesized rings are constituted by SWNTs closely packed in bundles. They contain from tens to hundreds of individual nanotubes, whose interaction are likely to control electronic pathways along the ring.

The study of these complex system is difficult due to the large number of involved carbon atoms. First, the bundle packing effect will be scrutinized (drawn on FIG. 5a). Our goal is to understand how relevant is the Van der Waals interaction between rings and how it affects the persistent current patterns. Second, following some experimental observations [13], in perfect torimade with a curled nanotube (as shown in FIG. 5b) will be under consideration. These two models allow to envision the bundle effect on large ring systems.

The study of persistent currents, when torus-torus interaction is turned on, is done by constructing a model of bundle. It consists in sticking two of these objects (namely A and B), and allowing them to interact with an ad hoc potential. This tube-tube hopping, that we call  $t_{ij}$ , was optimized to reproduce correctly the electronic properties of 3D graphite [37] or MWNTs [38]. Such a tube-tube interaction between two tori is believed to affect the shape or the intensity of  $I_{pc}(\phi)$  in various ways. The hamiltonian is now

$$H = H_A + H_B + \sum_{i,j} t_{ij} p_i^\dagger p_j + \sum_{i,j} p_i^\dagger p_j : \exp(i\phi'_{ij}) \quad (21)$$

$H_A$  and  $H_B$  are the hamiltonians (4) of the non-interacting rings, and  $p_i$  (resp.  $p_j$ ) is a  $p_z$ -orbital of the A (resp. B) torus. The phase  $\phi'_{ij}$  is given by (5) and

the secondary hopping integral is

$$t_1 = V_{\text{int}} \exp \frac{d}{l} \quad (22)$$

where  $d$  denotes the relative distance between the two sites. We take the value  $\epsilon_0 = 2.9$  eV, which allows the TB model to fit experimental data [39]. The other parameters are:  $V_{\text{int}} = 0.36$  eV,  $a = 3.34$  Å and  $l = 0.45$  Å. To simplify the comparison with precedent sections,  $\epsilon_0$  is kept as the energy unit.

It is important to note that the two subsystems are forced to have the same circumference, hence the field corresponding to  $\theta = \theta_0$  is the same in the two cases. If there are multiple correspondences between magnetic flux and field, and the  $\theta_0$ -periodicity is ill defined. As such situation may happens, we should avoid it to extract the effect of the tube-tube interaction. The choice of the subsystems is then restricted to equivalent helicities (e.g. two arm chair tubes, two zigzag tubes, two  $(3n, 2n)$ , etc.). The distance between the tube walls is fixed to  $a = 3.4$  Å.

Our calculations show first that a semiconducting tube has no effect on the persistent current of a metallic one. We can imagine the distribution of states of the interacting tori as two quasi-continua under interaction. The resulting quasi-continuum, which is the set containing all the eigenstates of the total system, is a mixing of the eigenstates of each non-interacting subsystem. However the mixing rate is proportional to  $(\epsilon_i - \epsilon_j)$ , where  $\epsilon_i$  and  $\epsilon_j$  are the two considered eigenvalues of each free torus. Hence, none coupling within the gap of the semiconducting torus happens. More, the persistent current in the metallic torus is carried by the levels around  $\epsilon_F$ , where the semiconducting tube does not have any state, then the persistent current of the complex system is equal to the persistent current of the free metallic torus.

The interesting cases arise whenever two metallic tori are interacting. The studied bundle is made with two  $(7, 7)$  tori containing 84 primitive cells (they are type I tori, with a degenerated Fermi level). By varying the relative orientations of the two tubes before curling them, and since the interaction  $t_1$  depends upon the geometry of the two subsystems, different cases of interaction schemes are explored. As shown on FIG. 6 a) and b), the tube-tube interaction induces a HOMO-LUMO gap at zero flux, and breaks level degeneracies. The flux-dependent evolution of the discrete levels shows that several crossing between eigenstates are driven by increasing magnetic flux, until the pattern returns to its original configuration when  $\theta = \theta_0$ . Since the value of the discrete energy levels changes from one orientation to another, the different level crossings induce modifications of the shape of  $I_{\text{pc}}(\Phi)$ . However the slope of the currents, which depends on the circumference and the Fermi velocity only, is unaffected. On FIG. 7 is shown the function  $I_{\text{pc}}(\Phi)$  for the two former cases and for the free tori is shown. Hence in all cases, the tube-tube interaction will reduce the typical persistent current when compared to the isolated torus.

Obviously, the precedent system is far to be a generic case, since the chosen torus is one of the highest symmetry. More, each subsystem is just the mirror



image of the other one. The effect of incommensurability is then addressed considering two different metallic SWNTs, with similar diameter (the (7;7) and (11;2) have same radii and the length cell of the latter is exactly seven times the length cell of the former). After checking that the magnetic properties of the (7;7) 84 torus are exactly the same than the (11;2) 12, the study of the bundle composed by one (7;7) torus containing 84 periods and one (11;2) torus containing 12 periods is made. In this case even though the ring is by definition  $L_{\text{ring}}$ -periodic ( $L_{\text{ring}} = 2.07$  nm here), the disorder-free bundle becomes quite different from the previous ones since there is now incommensurability at short scale. The resulting discrete levels are plotted as function of flux on FIG .6.c). Close to the charge neutrality, the evolution of the levels is very similar to those of the single torus. Then, in the incommensurate case, the tube-tube interaction is not able to open an HOMO-LUMO gap, and the persistent current (also shown in FIG .7) is roughly equivalent to twice the one of the free torus.

Consequently, in this case, the tube-tube interaction could act as a static disorder, with a modulation strength  $W = \hbar v_F \phi_0 = 10$ . As discussed in the previous part, this range of disorder induces no relevant perturbations on the persistent currents, and explain why the PC of non-commensurate tori are not affected by tube-tube interactions.

Finally, a last check is done. The FIG .6.d) shows the discrete levels of the (11;2) + (2;11) structure. The splitting of levels is present, and is of the same order of magnitude than that the (7;7) + (7;7) case. This means that the physical reason of absence of perturbation of PC is an effect of short range incommensurability and is not intrinsic to the underlying chirality.

## V Coiled nanotubes

In this part we are concerned with coiled nanotubes. These structures are imperfectly closed nanotori, which are rolled up with finite length nanotubes. The two ends of the nanotube are stucked through a Van der Waals interaction, like shown on FIG 5.b). The circumference of the curled system  $L_{\text{ring}}$  is necessary shorter than the length of the uncurled structure, otherwise sticking is impossible. The length of the sticking area is noted  $L_{\text{stick}}$ , while the distance between the two tube's ends is  $d_{\text{stick}}$ . Of course, these three parameters can vary within a given bundle, and depending on their relative values, different pattern of  $I_{\text{pc}}(\phi)$  will result.

If we keep restricting the working space to the  $p_z$  orbitals, the electronic hamiltonian takes the following expression

$$H = H_0 + \sum_{\langle ij \rangle} \sum_{\langle ip \rangle} t_{ij} p_j + p_i h_{ij} \quad (23)$$

with  $H_0$  the hamiltonian of the uncurled structure, and  $t_{ij}$  defined by equation (22). Now the sum runs for the orbitals  $j_i$  (resp.  $p_i$ ) located on the right (resp. left) extremity of the nanotube. Since the second part is clearly less important than the first it can be seen as a perturbation. This means that

the most relevant part of the hamiltonian describe an uncurled finite length nanotube. Such a kind of structures has been intensively investigated during the last years [40, 41, 42]. They exhibit a "particle-in-a-box" behavior which imply an important interplay between the total length  $L_{\text{ring}} + L_{\text{stick}}$ , chirality and HOMO-LUMO gap properties: the gap is zero when the Fermi moment is non-zero, and the number of primitive cells within the structure is  $3q + 1$  (i.e. corresponding to the type I tori), else the gap is non-zero (corresponding to the type II tori). The principal difference with the torus is that the rotational symmetry is lost, and the resulting electronic pathways around the ring are completely driven by the inter-tube hopping at the edges. The probability of hopping from one extremity to the other one will then depend on the geometry of the eigenstates around  $\Gamma$ , then upon the length and the chirality of the used nanotube.

Calculations were done on the (5,5) nanotube, with open ends. The parameter  $d_{\text{stick}}$  monitors the interlayer hopping value, since  $\gamma_1$  depends on the distance (equation (22)). As shown on FIG. 8 (top), the results show that the intensity of  $I_{\text{pc}}(\omega)$  is weakly dependent on the parameter  $d_{\text{stick}}$ , whereas the shape is not affected. The dependence on the sticking length  $L_{\text{stick}}$  is drawn on FIG. 8 (bottom), keeping  $L_{\text{ring}}$  constant, showing the resonances according to the "particle-in-a-box" model. The shape is strongly dependent on the length (or the number of unit cells) of the curled tube : adding one unit cell could switch the response from diamagnetic to paramagnetic, and if the length is resonant (the gap is minimal), the function  $I_{\text{pc}}(\omega)$  is quasi  $\omega_0=2$ -periodic. In all cases, the intensity of PCs is one order of magnitude lower than in the ideal case.

## V I Slater-Koster approach

Until now, our study of the electronic properties of nanotori was limited to  $p_z$  orbitals only. This approach is equivalent to the zone folding technique. We know that this model presents some discrepancies compared to more refined calculations. More precisely, the curvature needed to roll-up the sheet onto a tube, and the resulting  $\sigma$ -mixing are responsible of a gap opening in the band structure of all the non-arm chair metallic nanotubes, and for a slight shifting of the Fermi moment  $k_F$  of arm chair nanotubes, that keep a real metallic behavior. Although these modifications are not spectacular, they affect directly the states just around the Fermi level. Since these states are carrying the persistent current, we need to study  $I_{\text{pc}}(\omega)$  for nanotori described by a more accurate approach than the zone folding technique.

Calculations were done with an orthogonal tight-binding hamiltonian with Slater-Koster description of the hopping integrals. The parameters used are those of Louie and Tománek [43], but trials with Charlier, Gonze and Michenaud [44] parameters give the same results. The gap of metallic nanotubes is estimated  $\sim 0.106$  eV that is very large compared to the levels separation for zone folding method  $E_g = 2 \sqrt{E_F} = L$ . At the scale of this energy  $E_g$ , the

"metallic" nanotubes behave exactly like insulators : the magnetically induced current is small, as shown on FIG.9 for (9,0) based nanotorus.

However, the arm chair nanotubes preserve band crossings at Fermi level, which means that arm chair based nanotori (and only them) will still exhibit persistent currents. However, the Fermi momentum  $k_F$  is no more located at  $2/3$  of Brillouin zone, hence the concept of type I and II nanotori (with crossing of levels when  $\phi = 0$ , or not) loses its meaning. All the nanotori possess a non vanishing HOMO-LUMO gap for zero flux, and the crossing of levels does not happen exactly at the value  $\phi = \frac{2}{3}\phi_0$ . As a consequence, there are more level crossings at charge neutrality point within the  $[\phi_0=2; \phi_0=2]$ , as shown also on FIG.9, leading to a stronger weight of the higher harmonics in the Fourier spectrum. Compared to the zone folding results, we can then expect an increased sensitivity of the induced current, with temperature or disorder.

## V II conclusion and perspectives

In this work, a study of persistent current in nanotube based rings has been presented. It was first point out that disorder and temperature diminish the persistent currents in nanotori in a similar fashion as it does in 1D systems, assuming a Fermi energy at the charge neutrality point. Further, it has been established that tube-tube interaction does not affect the shape and intensity of  $I_{pc}(\phi)$ , except in the rare cases of commensurable systems.

On the other hand, the necessity of intertube hopping to convey electrons along a closed path was shown to weakly damp the magnitude of typical PCs. More, if the curvature induced spin mixing is taken into account in the model, then the persistent currents are completely screened, except for the arm chair based nanotori.

This suggests that such quantity may fluctuate significantly from one bundle to another and that it should be strongly reduced in regards to the specific pattern found in pure tori[45]. If, for some reasons (doping, etc...) the Fermi level is sufficiently shifted away from the charge neutrality point, then a linear dispersion relation is predicted for non-arm chair metallic tubes. Hence in this case, the persistent current may be as strong as the one of arm chair based nanotori.

This work is supported by European Community through the COMELCAN network (HPRN-CT-2000-00128). Pr. R. Saito and Pr. J. C. Charlier are acknowledged for valuable discussions.

## R eferences

- [1] R. Saito, G. Dresselhaus, and M. S. Dresselhaus, Physical properties of carbon nanotubes (Imperial College Press, London, 1998).
- [2] S. Tans, A. Verschueren, and C. Dekker, Nature 393, 49 (1998), A. Bach-told, P. Hadley, T. Nakanishi and C. Dekker, Science 294, 1317 (2001).

- [3] R. Martel, T. Schmidt, H. R. Shea, T. Hertel, Ph. Avoiris, Appl. Phys. Lett. 73, 2447 (1998), F. Leonard and J. Terso, Phys. Rev. Lett. 88, 258302 (2002), S. Heinze, J. Terso, R. Martel, V. Derycke, J. Appenzeller and Ph. Avoiris, Phys. Rev. Lett. 89, 106801 (2002), J. Appenzeller, J. Knoch, V. Derycke, R. Martel, S. Wind, Ph. Avoiris, Phys. Rev. Lett. 89, 126801 (2002).
- [4] C. White and T. Todorov, Nature 393, 240 (1998), T. Ando, Semicond. Sci. Technol. 15, R13 (2000).
- [5] S. Roche, G. Dresselhaus, M. Dresselhaus, and R. Saito, Phys. Rev. B 62, 16092 (2000), S. Roche and R. Saito, Phys. Rev. Lett. 87, 246803 (2001).
- [6] P. Poncharal, C. Berger, Y. Yi, Z. L. Wang, and Walt A. de Heer, J. Phys. Chem. 106, 12104 (2002).
- [7] S. Roche, F. Triozon, A. Rubio, and D. Mayou, Phys. Lett. A 285, 94 (2001),  
ibid, Phys. Rev. B 64, 121401 (2001).
- [8] H. Suzuura and T. Ando, Mol. Cryst. Liq. Cryst. 340, 731 (2000).
- [9] M. Bockrath, D. H. Cobden, J. Lu, A. G. Rinzler, R. E. Smalley, L. Balents, and P. L. McEuen, Nature 397, 598 (1999).
- [10] R. Egger, Phys. Rev. Lett. 83, 5547 (1999), E. Arrigoni, Phys. Rev. B 61, 7909 (2001), R. Egger and A. Gogolin, Phys. Rev. Lett. 87, 66401 (2001).
- [11] T. W. Odom, J.-L. Huang, P. Kim and C. M. Lieber, J. Phys. Chem. B 104, 2794 (2000).
- [12] J. Liu, H. Dai, J. H. Hafner, D. T. Colbert, R. E. Smalley, S. J. Tans, C. Dekker, Nature 385, 780 (1997).
- [13] R. Martel, H. R. Shea, and Ph. Avoiris, Nature 398, 299 (1999), ibid, J. Phys. Chem. B 103, 7551 (1999).
- [14] H. Watanabe, C. Manabe, T. Shigenatsu, and M. Shimizu, Appl. Phys. Lett. 78, 2928 (2001).
- [15] G. Cubemati, J. Yi, and M. Porto, Appl. Phys. Lett. 81, 850 (2002).
- [16] H. Shea, R. Martel, and Ph. Avoiris, Phys. Rev. Lett. 84, 4441 (2000).
- [17] C. Schonenberger, A. Bachtold, C. Strunk, J.-P. Salvetat and L. Forr, Appl. Phys. A 69, 283 (1999).
- [18] A. Fujiwara, K. Tomiyama, H. Suematsu, M. Yumura, K. Uchida, Phys. Rev. B 60, 13492 (1999).
- [19] F. London, J. Phys. Rad. 8, 397 (1937).

- [20] M . Buttiker, Y . Im ry, R . Landauer, Phys. Lett. A 96, 365 (1983), L . P . Levy, G . D olan, J . D unsm uir, and H . B ouchiat, Phys. Rev. Lett. 64, 2074 (1990).
- [21] N . Trivedi and D . A . Browne, Phys. Rev. B 38, 9581 (1988).
- [22] V . E . K ravtsov and B . L . A ltschuler, Phys. Rev. Lett. 84, 3394 (2000).
- [23] D . M ailly, C . Chapelier, and A . Benoit, Phys. Rev. Lett. 70, 2020 (1993).
- [24] V . Ambegaokar and U . Eckem, Phys. Rev. Lett. 65, 381 (1990).
- [25] T . G iam archi and B . S . Shastry, Phys. Rev. Lett. 51, 10915 (1995).
- [26] V . M . Appel, G . Chiappe, and M . J . Sanchez, Phys. Rev. Lett. 85, 4152 (2000).
- [27] D . Loss, Phys. Rev. Lett. 69, 343 (1992).
- [28] M . F . Lin and D . S . Chuu, Phys. Rev. B 57, 6731 (1998).
- [29] M . M arganska and M . Szopa, Acta Phys. Pol. B 32, 427 (2001).
- [30] In fact, there is a little modification of the energy, due to a magnetization  $M$  induced by the magnetic flux as  $M = \chi_m \Phi$ , where  $\chi_m$  is the magnetic susceptibility, equivalent to susceptibility of straight nanotube. However since this magnetisation do not exhibit any  $\Phi = 0$  behavior, we ignore it.
- [31] H . F . Cheung, Y . Gefen, E . K . R iedel, and W . H . Shih, Phys. Rev. B 37, 6050 (1988), there is an error in the legend of figure (3). The letter (a) labelizes actually the even number and (b) the odd.
- [32] P . W . Anderson, Phys. Rev. 109, 1492 (1958).
- [33] Y . Im ry, Introduction to mesoscopic physics (Oxford University Press, New York, 1997).
- [34] H . Cheung, E . K . R iedel, and Y . Gefen, Phys. Rev. Lett. 62, 587 (1989).
- [35] H . Bouchiat and G . Montambaux, J. Phys. France 50, 2695 (1989), G . Montambaux, H . Bouchiat and R . Friesner, Phys. Rev. B . 42, 7647 (1990).
- [36] A . Altland, Y . Gefen, and G . Montambaux, Phys. Rev. Lett. 76, 1130 (1996).
- [37] J . C . Charlier, J . P . Michenaud, and P . Lambin, Phys. Rev. B 46, 4540 (1992).
- [38] P . Lambin, V . Meunier, and A . Rubio, Phys. Rev. B 62, 5129 (2000).
- [39] G . Dresselhaus et al., On the overlap energy in carbon nanotubes in "Science and Application of Nanotubes", D . Tom anek and R . J . Enbody ed. (Kluwer Academic, New-York, 2000).

- [40] L. Liu, C. S. Jahanthi, H. Guo, and S. Y. Wu, Phys. Rev. B 64,033414 (2000).
- [41] A. Rochefort, D. R. Salahub, and P. A. Vouris, J. Phys. Chem. B 103, 641 (1999).
- [42] A. Rubio, D. Sánchez-Portal, E. Artacho, P. Ordeñ, and J. M. Soler, Phys. Rev. Lett. 82, 3520 (1999).
- [43] D. Tománek and S. G. Louie, Phys. Rev. B 37, 8327 (1988).
- [44] J.-C. Charlier, X. Gonze, and J.-P. Michenaud, Phys. Rev. B 43, 4579 (1991), P. Lambin, L. Philippe, J. C. Charlier and J. P. Michenaud, Comput. Mater. Sci. 2, 350 (1994)
- [45] L. Liu, G. Guo, C. Jayanthi, and S. Wu, Phys. Rev. Lett. 88, 217206 (2002), S. Latil, S. Roche, A. Rubio and P. Lambin, comment submitted in Phys. Rev. Lett.

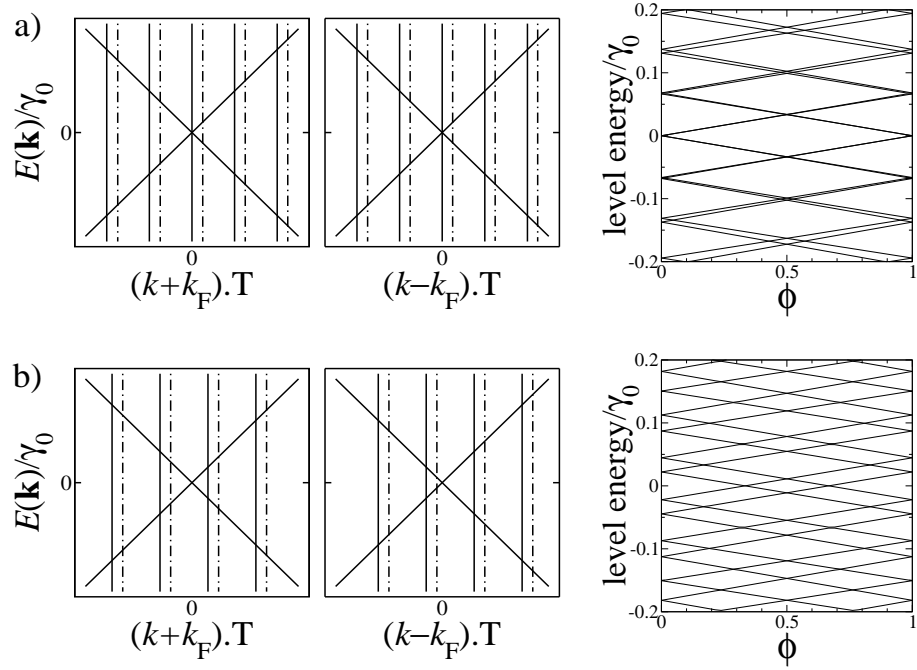


Figure 1: The cyclic boundary conditions in the nanotorus produces a confinement, responsible of the sampling of the first Brillouin zone of the SW NT. At left a zoom of the vicinity of the crossing points is drawn, the vertical solid lines represent the sampling at zero flux, and the dot-dashed lines the sampling for a non-zero flux. At right, the resulting discrete electronic levels is plotted as a function of the dimensionless flux  $\phi$ . a) The HOMO-LUMO gap of the type I nanotorus vanishes at zero flux. Application of a magnetic field opens a gap by shifting the sampling of points. b) The pattern for the type II is more involved since two crossing of levels occurs during the evolution of the flux.

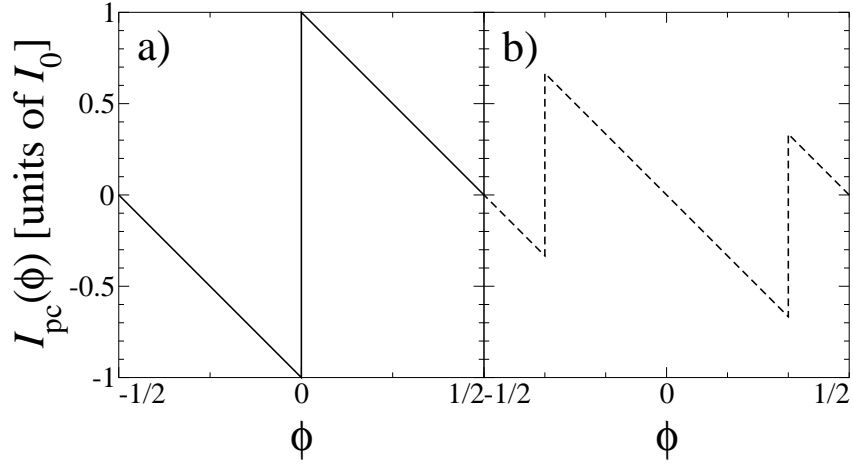


Figure 2:  $I_{pc}(\phi)$  for the two cases I (a) and II (b). The origin of the diamagnetic-paramagnetic transitions are the crossing of levels seen on FIG. 1.  $I_0$  is given by (11).

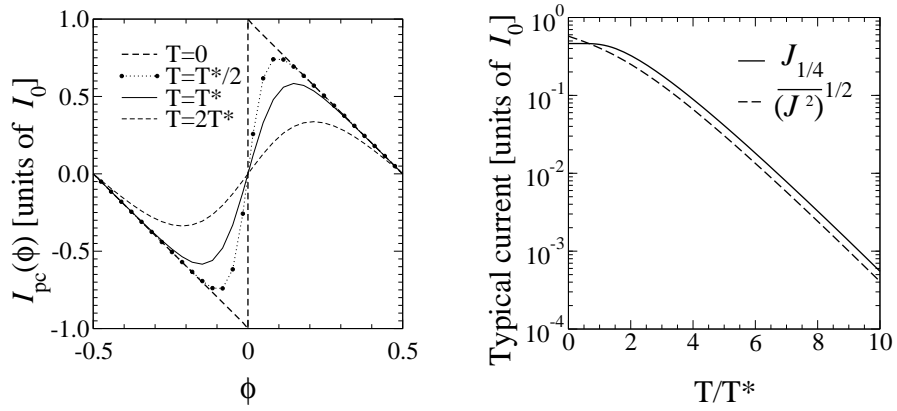


Figure 3: Left : Temperature effect on the persistent  $I_{pc}(\phi)$ . Right : Semilog plot of the temperature dependent typical currents. As it happens for the linear chain of atoms [31], these currents exhibit a transition temperature, namely  $T^*$  (see text), from which the intensity decreases exponentially.



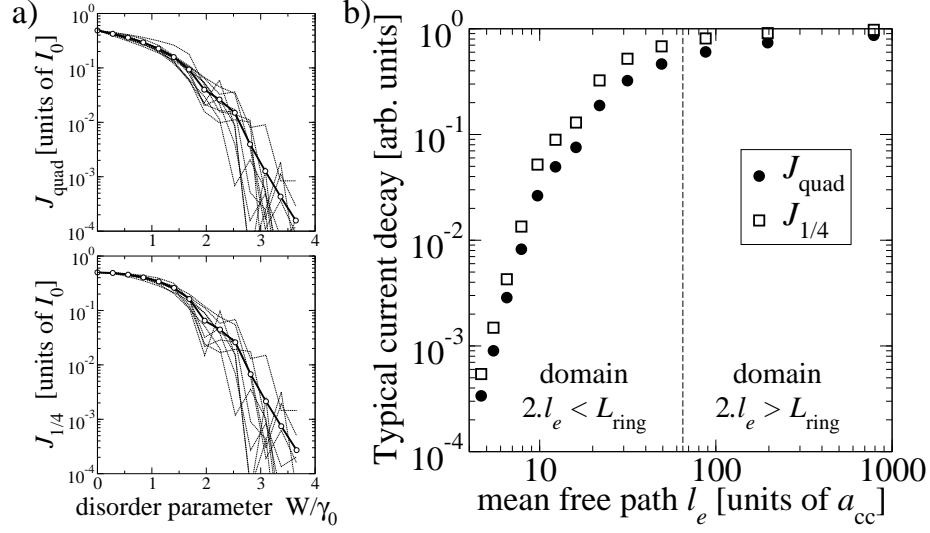


Figure 4: a) Semilog plot of the typical currents  $J_{\text{quad}}$  (up) and  $J_{1/4}$  (bottom) versus the disorder strength. The dashed lines describe different disorder configurations, their average is identified by the bold line with circles. b) Log-log plot of the typical currents as function of mean free path  $l_e$ , given by equation (18). The transition from a ballistic (small  $W$ , long  $l_e$ ) to a more localized (larger  $W$ , short  $l_e$ ) is pointed out by a vertical line, at which  $W$  yields  $L_{\text{ring}} = 2.l_e$ .

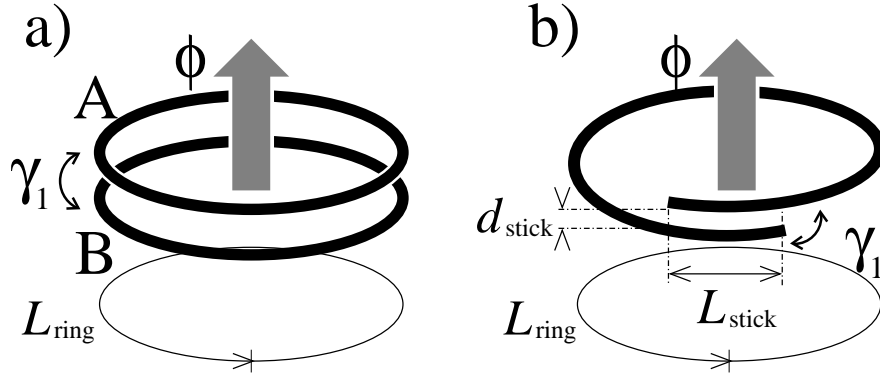


Figure 5: a) A complex ring made of two interacting carbon nanotubes. b) A coil-shaped carbon nanotube.

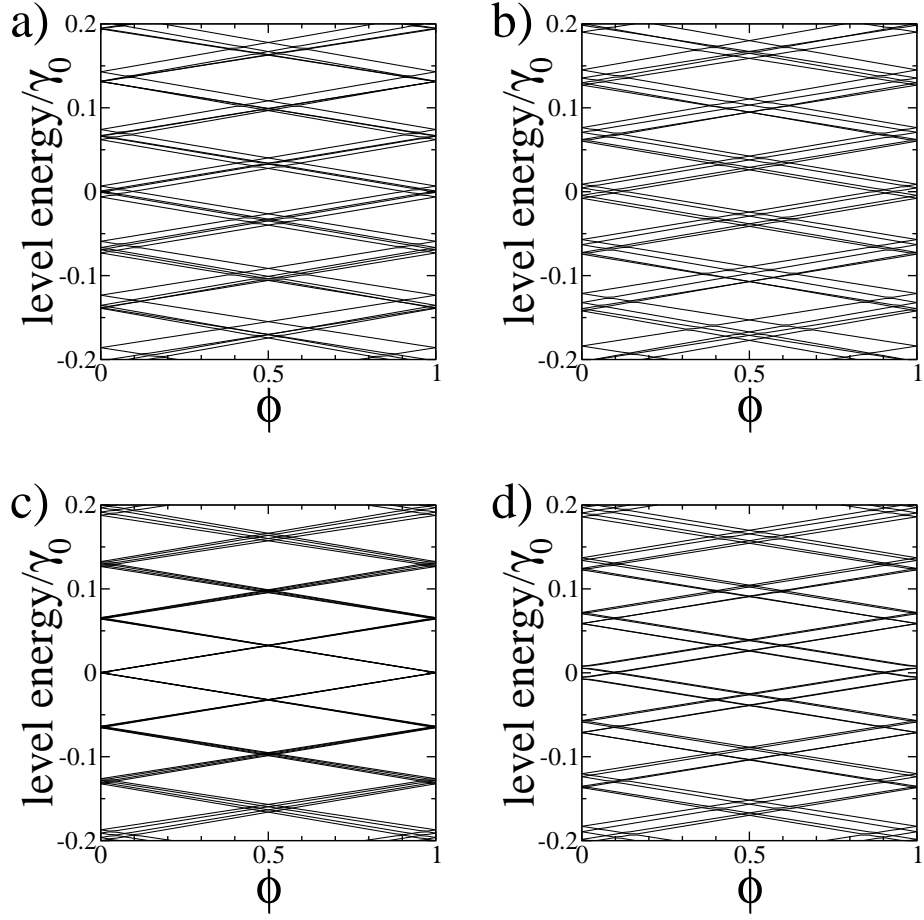


Figure 6: Discrete levels of two interacting tori, as function of flux. a) Two  $(7;7)$  84 tori. The tube-tube interaction induces a lifting of degeneracies. b) Two  $(7;7)$  84 tori, with different orientation. c) A  $(7;7)$  84 +  $(11;2)$  12 non commensurate system. It is fairly similar to the non-interacting case (see FIG. 1). d) A  $(11;2)$  12 +  $(2;11)$  12 commensurate system.

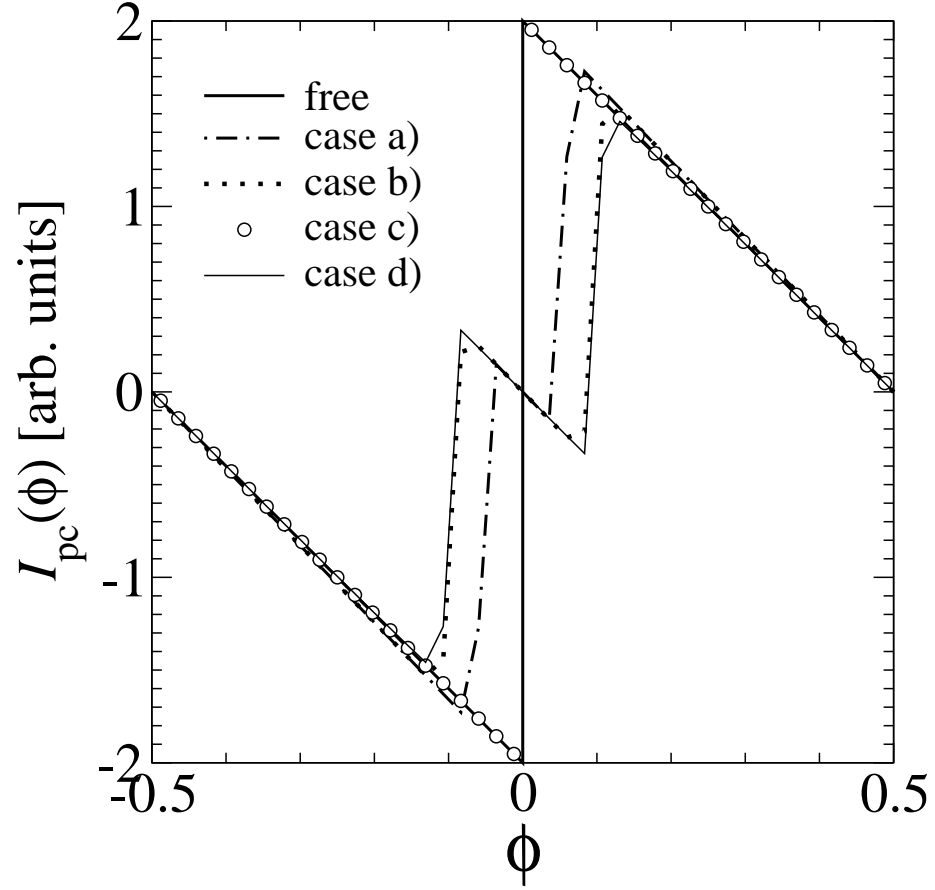


Figure 7: Flux dependent persistent currents, for the same cases than FIG .6. The shape  $I_{pc}(\phi)$  for the case a), b) and d) is due to the crossing of levels at Fermi energy. The non-commensurate structure (case c) behaves similarly than the free tori.

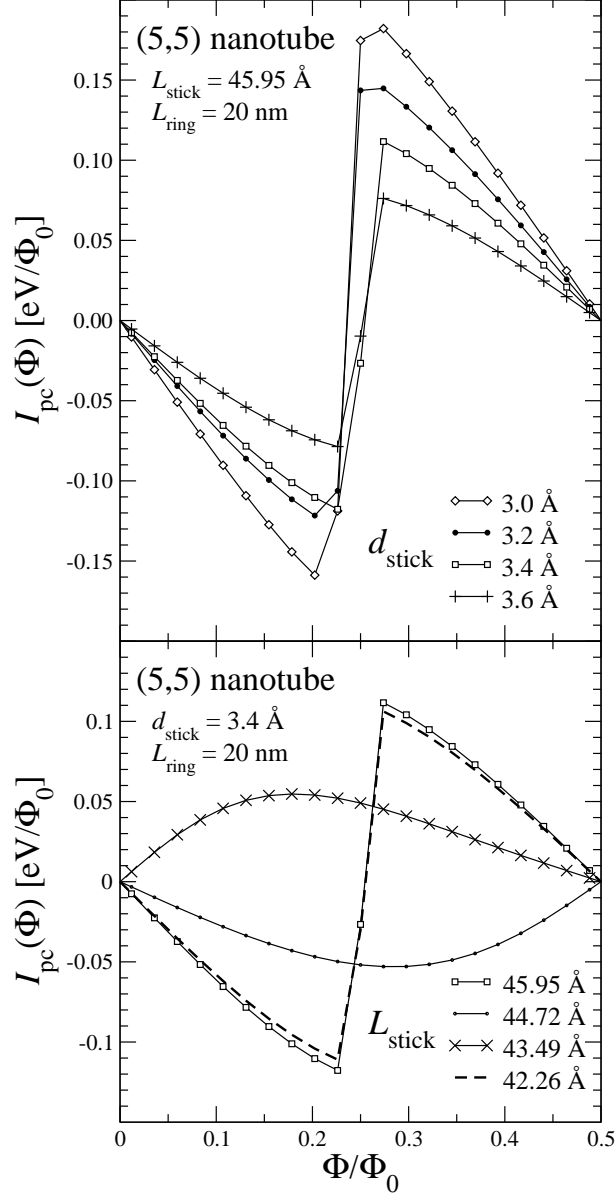


Figure 8: Flux dependent persistent currents induced in coiled nanotubes. Top: Evolution with respect to  $d_{\text{stick}}$  for fixed  $L_{\text{stick}}$  and  $L_{\text{ring}}$ . Bottom: Illustration of the effect of increasing  $L_{\text{stick}}$  while keeping  $L_{\text{ring}}$  and  $d_{\text{stick}}$  unchanged.

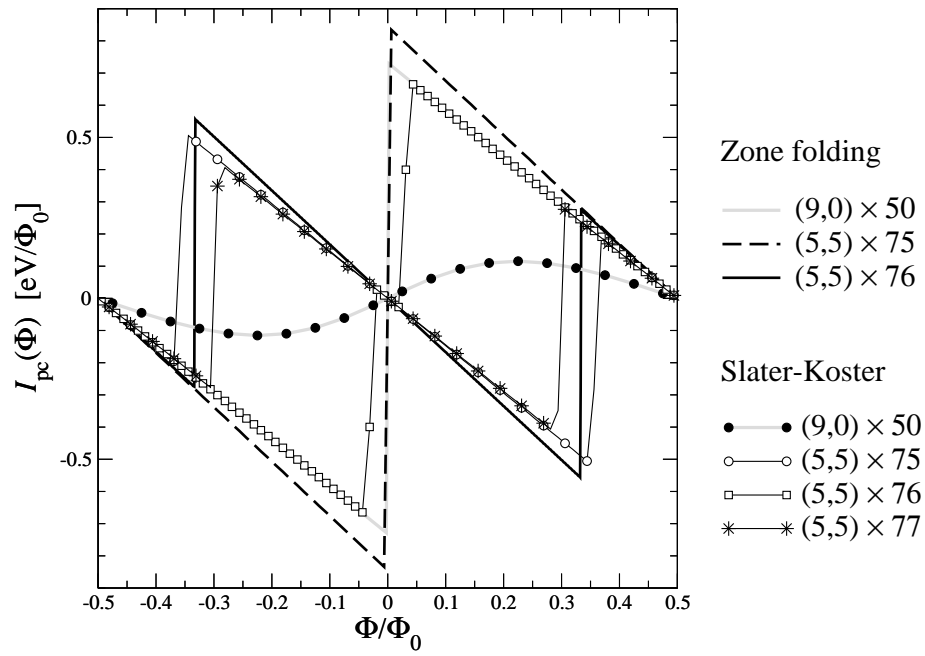


Figure 9: Comparison of persistent currents obtained for the (9,0) nanotube with the zone-folding method (thin lines) and the Slater-Koster approach (thick lines).